Cadmium Benzenethiolate Clusters of Various Size: Molecular Models for Metal Chalcogenide Semiconductors

Thomas Türk,[†,‡] Ute Resch,[‡] Marye Anne Fox,*[,‡] and Arnd Vogler*[,†]

Institut für Anorganische Chemie, Universität Regensburg, Universitätsstrasse 31, W-8400 Regensburg, FRG, and Department of Chemistry, University of Texas, Austin, Texas 78712-1167 *(Received: December 26, 1991)*

The optical and electrochemical properties of three cadmium benzenethiolate clusters, $Cd(SPh)_4^{2-}$, $Cd_4(SPh)_{10}^{2-}$, and $Cd_{10}S_4(SPh)_{16}^{4-}$, are studied as function of the cluster size. The Cd_n clusters (n = 1, 4, 10) which may represent molecular models for the semiconductor CdS show structured absorption spectra that are assigned to both ligand-to-metal charge-transfer (LMCT) and intraligand transitions. The absorption and emission bands of Cd_{10} are red-shifted compared to those of Cd_1 and Cd_4. The emission of the Cd_n clusters (n = 4, 10) is ascribed to a LMCT transition as suggested by the short luminescence lifetimes and the red shift with increasing cluster size. Illumination of the Cd_n clusters yields thianthrene, dibenzothiophene, and benzenethiol, the rate of photodegradation depending on the cluster size. Electrochemical studies of Cd_n show that, with increasing cluster size, the oxidation potential is shifted negative while the reduction potential is shifted positive. Both Cd_4 and Cd_{10} form charge-transfer complexes with methyl viologen. However, steady-state illumination of these clusters in the presence of methyl viologen does not result in the formation of the methyl viologen radical cation.

Introduction

The electronic properties of bulk inorganic semiconductors are collective properties that result from the periodic arrangement of a large number of atoms or molecules in a crystal lattice. As the diameter of the semiconductor crystallite is successively decreased in the nanometer range, a gradual transition from the bulk semiconductor to the properties of very small particles (size quantization effect) occurs.[1-5] This transition leads to substantial changes in both the optical and photocatalytic properties,[1-5] as well as in the electrochemical behavior.[6] A further reduction of the crystallite size finally yields molecular dimensions.

Several approaches involving colloidal semiconductors have been described in order to observe the transition region between semiconductor and molecular properties.[1-13] However, the relatively broad particle size distribution of most colloids complicates the quantitative correlation of the photophysical properties of the semiconductor with the crystallite size. Such a correlation is improved through rigorous control of the semiconductor particle size and dispersity. New methods for preparing and isolating semiconductor crystallites with a very narrow size distribution have been recently developed involving the synthesis of particles in vesicles,[7] zeolites,[8] and polymers,[9] surface modification procedures,[10,11] biosynthesis,[12] and separation (according to size) by chromatography.[13] The synthesis of monodisperse inorganic clusters of various sizes represents another approach.[14-18] The advantage of these synthetic clusters over conventional semiconductor colloids is their well-defined size[14-18] and structure.[14,16,17] Furthermore, molecular properties such as structural rearrangements in the excited state are observed in these species.

Suitable candidates for the investigation of molecular clusters are polynuclear cadmium benzenethiolate complexes such as $Cd(SPh)_4^{2-}$, $Cd_4(SPh)_{10}^{2-}$, and $Cd_{10}S_4(SPh)_{16}^{4-}$. The crystal structures of these Cd_n clusters (n = 1, 4, 10)[16] imply that they are well-suited as molecular models for CdS, one of the best studied semiconductors.[7a,8,9a,10,11d,12,13] Many structural features, i.e., the coordination environment of Cd and S, the Cd-S and Cd-Cd bond distances, and bond angles,[3,16,19] are very similar in the clusters and in the bulk semiconductor.

According to these considerations the optical properties of molecular clusters of this type should be of considerable interest. We explored this possibility and selected the clusters $Cd_{10}S_4(SPh)_{16}^{4-}$, $Cd_4(SPh)_{10}^{2-}$, and $Cd(SPh)_4^{2-}$ as reference compounds for the present study. In addition, some relevant observations on the electrochemistry and photochemistry are also reported.

[†] Universität Regensburg.
[‡] University of Texas.

Experimental Section

Materials. Benzenethiol, cadmium nitrate tetrahydrate, triethylamine, tributylamine, tetramethylammonium chloride, sulfur, tetrabutylammonium hexafluorophosphate, methyl viologen di-

(1) (a) Henglein, A. *Top. Curr. Chem.* **1988**, *143*, 113-180. (b) Henglein, A. *Chem. Rev.* **1989**, *89*, 1861-1873.
(2) (a) Brus, L. E. *J. Phys. Chem.* **1986**, *90*, 2555-2560. (b) Steigerwald, M. L.; Brus, L. E. *Acc. Chem. Res.* **1990**, *23*, 183-188.
(3) Wang, Y.; Herron, N. *J. Phys. Chem.* **1991**, *95*, 525-532.
(4) Stucky, G. D.; MacDougall, J. E. *Science* **1990**, *47*, 669-678.
(5) Fox, M. A. *Res. Chem. Intermed.* **1991**, *15*, 153.
(6) Leland, J. K.; Bard, A. J. *J. Phys. Chem.* **1987**, *91*, 5083-5087.
(7) (a) Watzke, H. J.; Fendler, J. H. *J. Phys. Chem.* **1987**, *91*, 854-860. (b) Chang, A.-C.; Pfeiffer, W. F.; Guillaume, B.; Baral, S.; Fendler, J. H. *J. Phys. Chem.* **1990**, *94*, 4284-4289.
(8) (a) Wang, Y.; Herron, N. *J. Phys. Chem.* **1988**, *92*, 4988-4994. (b) Herron, N.; Wang, Y.; Eddy, M. M.; Stucky, G. D.; Cox, D. E.; Moller, K.; Bein, T. *J. Am. Chem. Soc.* **1989**, *111*, 530-540.
(9) (a) Kakuta, N.; White, J. M.; Campion, A.; Bard, A. J.; Fox, M. A.; Webber, S. E. *J. Phys. Chem.* **1985**, *89*, 48-52. (b) Wang, Y.; Suna, A.; Mahler, W.; Kasowski, R. *J. Chem. Phys.* **1987**, *87*, 7315-7322.
(10) (a) Dannhauser, T.; O'Neil, M.; Johansson, K.; Whitten, D.; McLendon, G. *J. Phys. Chem.* **1986**, *90*, 6074-6076. (b) Spanhel, L.; Haase, M.; Weller, H.; Henglein, A. *J. Am. Chem. Soc.* **1987**, *109*, 5649-5055. (c) Wang, Y.; Suna, A.; McHugh, J.; Hilinski, E. F.; Lucas, P. A.; Johnson, R. D. *J. Chem. Phys.* **1990**, *92*, 6927-6939.
(11) (a) Steigerwald, M. L.; Alivisatos, A. P.; Gibson, J. M.; Harris, T. D.; Kortan, R.; Muller, A. J.; Thayer, A. M.; Duncan, T. M.; Douglass, D. C.; Brus, L. E. *J. Am. Chem. Soc.* **1988**, *110*, 3046-3050. (b) Nosaka, Y.; Yamaguchi, K.; Miyama, H. *Chem. Lett.* **1988**, 605-608. (c) Kortan, A. R.; Hull, R.; Opila, R. L.; Bawendi, M. G.; Carroll, P. J.; Brus, L. E. *J. Am. Chem. Soc.* **1990**, *112*, 1327-1332. (d) Herron, N.; Wang, Y.; Eckert, H. *J. Am. Chem. Soc.* **1990**, *112*, 1322-1326.
(12) Dameron, C. T.; Reese, R. N.; Mehra, R. K.; Kortan, A. R.; Carroll, P. J.; Steigerwald, M. L.; Brus, L. E.; Winge, D. R. *Nature* **1989**, *338*, 596-597.
(13) (a) Fischer, Ch.-H.; Weller, H.; Fojtik, A.; Lume-Pereira, C.; Janata, E.; Henglein, A. *Ber. Bunsen-Ges. Phys. Chem.* **1986**, *90*, 46-49. (b) Fischer, Ch.-H.; Lilie, J.; Weller, H.; Katsikas, L.; Henglein, A. *Ber. Bunsen-Ges. Phys. Chem.* **1989**, *93*, 61-64. (c) Fischer, Ch.-H.; Weller, H.; Katsikas, L.; Henglein, A. *Langmuir* **1989**, *5*, 429-432. (d) Eychmueller, A.; Katsikas, L.; Weller, H. *Langmuir* **1990**, *6*, 1605-1608.
(14) Lacelle, S.; Stevens, W. C.; Kurtz, D. M.; Richardson, J. W.; Jacobson, R. A. *Inorg. Chem.* **1984**, *23*, 930-935.
(15) Dean, P. A. W.; Vittal, J. J. *Inorg. Chem.* **1986**, *25*, 514-519.
(16) Dance, I. G.; Choy, A.; Scudder, M. L. *J. Am. Chem. Soc.* **1984**, *106*, 6285-6295.
(17) Brennan, J. G.; Siegrist, T.; Stuczynski, S. M.; Steigerwald, M. L. *J. Am. Chem. Soc.* **1990**, *112*, 9233-9236.
(18) Kunkely, H.; Vogler, A. *J. Chem. Soc., Chem. Commun.* **1990**, 1204-1205.
(19) *Gmelins Handbuch der Anorganische Chemie*; Verlag Chemie GmbH: Weinheim, 1959; p 596.

0022-3654/92/2096-3818$03.00/0

chloride hydrate, thianthrene, and dibenzothiophene were used as received from Aldrich. All photochemical studies were carried out with spectroscopic grade solvents. The Cd_n clusters (n = 1, 4, 10) were synthesized following the procedure described by Dance et al.[16] and characterized by elemental analysis and FTIR spectroscopy. Methyl viologen was used as a perfluorophosphate salt.

Methods. Absorption spectra were recorded on a Hewlett-Packard 8451A single-beam spectrophotometer. Steady-state luminescence spectra were measured on an SLM Aminco 500 C spectrofluorometer. For emission measurements at room temperature, solutions of Cd_n in CH_3CN were used, whereas luminescence measurements at 77 K were carried out with Cd_n in the solid state (powders). Photolysis of Cd_n in CH_3CN was carried out with a 1000-W high-pressure mercury lamp. The lamp intensity was attenuated by using calibrated metal screens. High-resolution mass spectra (EI) were recorded on a VG Analytical mass spectrometer (ZAB 2-E). The photolyzed Cd_n solutions were evaporated to dryness and directly analyzed by mass spectroscopy (MS). Electrochemical measurements were performed with a Princeton Applied Research 175 universal programmer and a Model 173 potentiostat. The signal was recorded on a Houston Instruments 2000 X–Y recorder. A conventional single-compartment electrochemical cell equipped with either a Pt disk (oxidation) or a hanging mercury drop electrode (HMDE) (reduction), working electrode, a Pt wire counter electrode, and a Ag/AgCl reference electrode was used. Tetrabutylammonium hexafluorophosphate (0.13 M) was used as supporting electrolyte and spectrograde CH_3CN (dried over molecular sieves) as solvent. All electrochemical studies were carried out under N_2.

Time-resolved emission measurements with Cd_n (n = 4, 10) in CH_3CN were performed via time-correlated single photon counting (SPC) using a mode-locked frequency-doubled Nd:YAG laser (Quantronix Model 416) synchronously pumping a cavity-dumped dye laser (Coherent Model 701-3D; Rhodamine 6G). The dye laser output (at 586 nm) was frequency doubled using an angle-tuned KDP crystal to produce pulses at 293 nm. The instrument response function was ca. 70 ps fwhm (full width at half-height of the maximum). The decay profiles were fit to a multi-exponential decay function using standard least-squares deconvolution techniques. The shortest lifetime which could be determined was 25 ps. The quality of the fits was evaluated by χ^2 test and the randomness of the distribution of the residuals. The emissions of Cd_4 and Cd_{10} were monitored at 500 and 545 nm, respectively. All measurements were carried out with air-saturated solutions at room temperature. For each luminescence lifetime, an average deviation of ±5% was observed.

The luminescence lifetimes of the Cd_n powders were measured at 77 K using the transient diffuse reflectance spectroscopic technique. The samples were excited at 266 nm with a frequency-quadrupled Nd:YAG laser (pulse width 11 ns).

Results and Discussion

Absorption Spectra of Cd_1, Cd_4, and Cd_{10}. The absorption spectra of Cd_n in CH_3CN are shown in Figure 1. Cd_1, which contains only terminal benzenethiolate ligands, exhibits an absorption band at 282 nm (ϵ_{282} = 20 300 M^{-1} cm^{-1}), whereas two maxima are observed for both Cd_4 (275 nm (ϵ_{275} = 115 900 M^{-1} cm^{-1} and 249 nm (ϵ_{249} = 117 400 M^{-1} cm^{-1}))[20] and Cd_{10} (292 nm (ϵ_{292} = 138 200 M^{-1} cm^{-1}) and 255 nm (ϵ_{255} = 178 400 M^{-1} cm^{-1})). Cd_4 and Cd_{10} consist of two different types of benzenethiolate ligands, i.e., bridging and terminal benzenethiolates.[16] Each bridging benzenethiolate ligand is bound to two Cd atoms via the lone electron pair of the benzenethiolate sulfur, whereas the terminal benzenethiolates are attached to one Cd. The pure ligand, benzenethiolate (303 nm; ϵ_{303} = 13 600 M^{-1} cm^{-1}),[21] displays a significantly different absorption spectrum. For related anionic ligands such as phenolate, coordination with the lone electron pair is usually accompanied by a blue-shift of the intraligand absorption bands.[22] Cd_{10} additionally, contains some S^{2-} ligands.[16] However, the absorption spectra of the Cd_n clusters are most likely a composite of intraligand and ligand-to-metal charge-transfer (LMCT) transitions. Since S^{2-} and SPh^- have certainly very similar electronegativities (S^{2-} to and SPh^- to Zn^{2+}), LMCT transitions should occur at comparable energies.[23] A LMCT assignment is further supported by the apparent metal-to-ligand charge-transfer (MLCT) emission of Cd_4 and Cd_{10}. (See emission spectra and lifetimes below.)

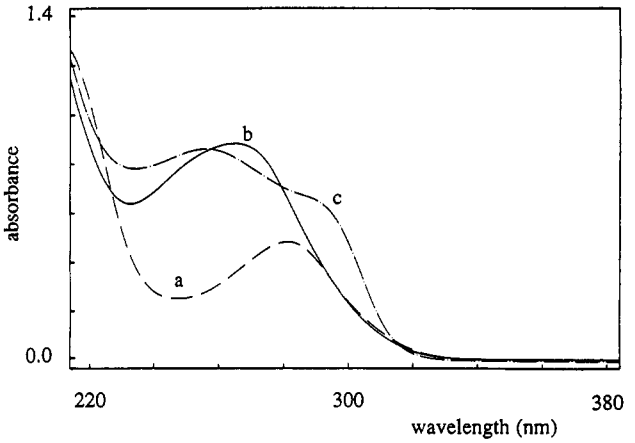

Figure 1. Absorption spectra of (a) 2.5 × 10^{-5} M Cd_1, (b) 6.9 × 10^{-6} M Cd_4, and (c) 4.9 × 10^{-6} M Cd_{10} in CH_3CN at room temperature (1-cm cell).

For a series of mononuclear alkyl thiolate complexes of cadmium, absorption spectra similar to that of Cd_1 showing a broad absorption band in the 240–290-nm region with extinction coefficients in the 30 000–40 000 M^{-1} cm^{-1} range have been previously reported.[24] The absorption bands of these alkyl thiolate complexes were assigned to LMCT transitions.[24]

The bulk semiconductor CdS has a band gap of 2.4 eV (onset of absorption, λ_{os} = 516 nm).[25] In a molecular picture, this band gap transition can be also regarded as a LMCT transition since the filled sulfide 3p valence orbitals form the valence band of CdS, whereas its conduction band is composed of the empty Cd^{2+} 5s orbitals.[18,26] The number of interacting sulfide and Cd^{2+} orbitals affects the energy of the band gap, or LMCT transition, in such a way that an increase in the number of interacting atoms, i.e., an increase in the crystallite size, leads to a red-shift of the band gap or LMCT transition.[3,26] $(Cd_{20}S_{13}(SPh)_{22})^{8-}$, a 55-atom 10-Å cluster, may be the smallest cadmium–sulfur cluster yet reported which is assumed to show both the bulk sphalerite structure and a sharp absorption band at 351 nm.[3] A further growth of the crystallite causes a steady bathochromic shift of both the absorption onset and the luminescence as shown for thiophenol-capped size-quantized CdS particles.[11d]

The absorption spectra of the polynuclear Cd_n clusters (n = 4, 10) reported here are clearly affected by the size of the cluster; i.e., the absorption maxima of Cd_{10} are red-shifted compared to those of Cd_4. A similar size dependence is also observed for the emission spectra of Cd_n (see emission spectra below). In agreement with the qualitative model described above, this red-shift may be attributed to an increase in cluster size.[1-4]

(20) The positions of the maxima are determined from the second derivative of the absorption spectrum of Cd_4.

(21) Thiophenolate is obtained by deprotonation of benzenethiol with sodium hydroxide in CH_2CN under N_2.

(22) Calvert, J. G.; Pitts, J. N. *Photochemistry*; John Wiley & Sons: New York, 1967; pp 261–264.

(23) (a) The electronegativity of SPh^- is not known but assumed to be rather similar to that of S^{2-} (2.5) since the electronegativities of $NO_2C_6H_4S^-$ and $C_6F_5S^-$ with certainly electron-withdrawing substituents are slightly higher (2.9). (b) Lever, A. B. P. *Inorganic Electronic Spectroscopy*; Elsevier: Amsterdam, 1984; p 222.

(24) Carson, C. K.; Dean, P. A. W.; Stillman, M. J. *Inorg. Chim. Acta* **1981**, *56*, 59–71.

(25) *Landolt-Bernstein*; Springer-Verlag: Berlin, 1982; Vol. 17b, p 166.

(26) Bahnemann, D. W.; Kormann, C.; Hoffmann, M. R. *J. Phys. Chem.* **1987**, *91*, 3789–3798.

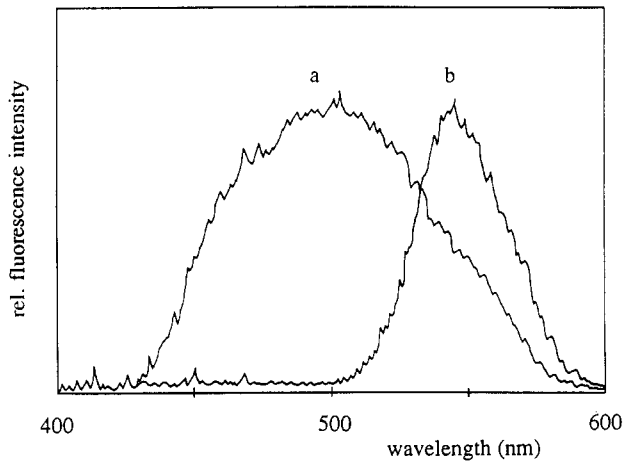

Figure 2. Uncorrected emission spectra of (a) 4.3×10^{-6} M Cd_4 and (b) 1.8×10^{-6} M Cd_{10} in aerated CH_3CN at room temperature (1-cm cell, excitation 310 nm).

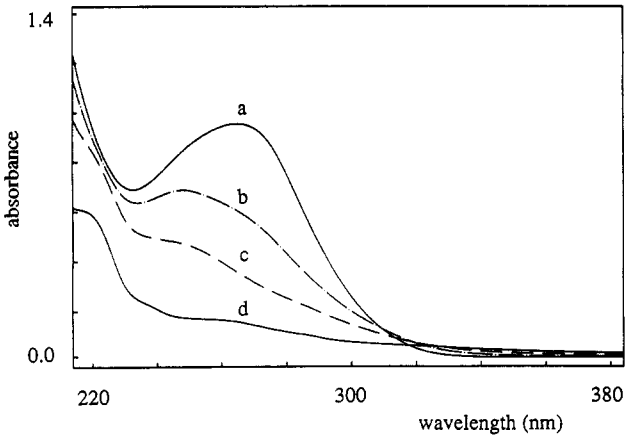

Figure 3. Photolysis of 7.4×10^{-6} M Cd_4 in CH_3CN in aerated solution. The absorption spectra were obtained after different illumination times: (a) before photolysis, (b) after 2 min, (c) after 5 min, and (d) after 60 min.

Emission Spectra and Lifetimes of Cd_4 and Cd_{10}. Both Cd_4 and Cd_{10} exhibit a very weak emission in CH_3CN at room temperature, both in deaerated solution and under air (Figure 2). Cd_1 shows no measurable emission. The luminescence spectra of the clusters are independent of the excitation wavelength. With increased cluster size,[1-4] the emission of Cd_{10}[27] (maximum at 545 nm) red-shifts from that of Cd_4 (maximum at 500 nm). The luminescence spectra of Cd_4 and Cd_{10} (Figure 2) show substantial Stokes shifts, indicating a large excited-state distortion. A similar Stokes shift of the emission was observed for tetranuclear clusters of other d^{10} metals: Cu^I, Ag^I, Au^I, Hg^{II}, and Zn^{II}.[18,28]

At 77 K, Cd_4 and Cd_{10} powders also display intense, broad emission bands at 465 and 455 nm, respectively. At 77 K, emission lifetimes of 1 μs are obtained for both clusters by transient diffuse reflectance spectroscopy. The long-lived emission at 77 K, which does not undergo a red-shift with cluster growth as is predicted theoretically for LMCT transitions,[3,26] is assigned to an (forbidden) intraligand transition. Benzenethiol is reported to show a low-temperature phosphorescence at 425 nm.[29] The longer wavelength emissions at room temperature were not detected at 77 K as they were obscured by the very intense intraligand bands.

For Cd_4 and Cd_{10} at room temperature, luminescence lifetimes of 390 and 590 ps, respectively, are determined by SPC. For both clusters, the emission at room temperature is ascribed to an (allowed) MLCT transition as suggested by both the short lifetimes and the red-shift of the emission bands with increasing cluster size.

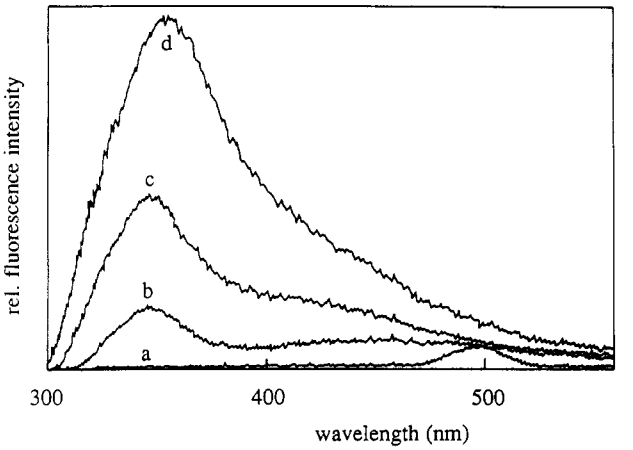

Figure 4. Photolysis of 7.4×10^{-6} M Cd_4 in CH_3CN in aerated solution. The uncorrected emission spectra were obtained after different illumination times: (a) before photolysis (×14), (b) after 2 min (×7), (c) after 5 min (×4), and (d) after 60 min. Excitation was always at 290 nm. The observed changes in luminescence intensity may be caused by both an inner filter effect and different luminescence quantum yields of the photoproducts.

Photodecomposition of Cd_1, Cd_4, and Cd_{10}. Illumination of Cd_4 in CH_3CN leads to a strong decrease of the absorption bands with time (Figure 3). Concomitantly, the luminescence of the cluster at 500 nm disappears and a new broad emission band with a maximum at 355 nm and a shoulder at 440 nm occurs (Figure 4). Oxygen does not influence the photodecomposition of the Cd_4 cluster: nearly identical decomposition rates are obtained with N_2, air, and O_2-saturated solutions. Furthermore, the short luminescence lifetimes of Cd_4 and Cd_{10} imply that a bimolecular photoreaction with O_2 should not occur.

Cd_1 and Cd_{10} exhibit photochemical behavior similar to Cd_4, and the same photoproducts are most likely obtained for all the Cd_n clusters as suggested by the similar absorption (Figure 3, spectrum d) and luminescence spectra (Figure 4, spectrum d) observed at long illumination times. However, the photodecomposition rates of the Cd_n clusters, i.e., their photostability, are clearly affected by cluster size: Cd_4 decomposes twice as fast as Cd_{10}, and photodegradation of Cd_1 is ca. 10 times faster than that of Cd_{10}.[30] This effect may be attributed to a higher degree of electronic delocalization in the bigger cluster, i.e., less probability of bond cleavages in the series Cd_1, Cd_4, Cd_{10}.

Interestingly, in the case of the Cd_n clusters, oxygen does not influence the photodecomposition, in contrast to previous observations with colloidal CdS which undergoes photocorrosion only in the presence of oxygen yielding H_2O_2, SO_4^{2-}, and Cd^{2+}.[31] However, most studies involving colloidal CdS were carried out in water, not in organic solvents such as CH_3CN.[31] In fact, photolysis of alkanethiol-capped CdS in tetrahydrofuran leads to dissolution of the colloid in aerated solution, whereas in the absence of oxygen larger particles and cadmium metal are formed.[32] In both cases, the photochemical formation of the corresponding disulfide (with the same rate) is observed.[32]

Analysis of the products formed from the illuminated Cd_n solutions by mass spectroscopy (MS) indicates the formation of thianthrene (m/e = 216), dibenzothiophene (m/e = 184), and benzenethiol (m/e = 110),[33] which were formed in comparable

(27) For Cd_{10} in CH_3CN, a similar emission at 530 nm has been reported by Herron et al.[11d]

(28) (a) Vogler, A.; Kunkely, H. *J. Am. Chem. Soc.* **1986**, *108*, 7211-7212. (b) Vogler, A.; Kunkely, H. *Chem. Phys. Lett.* **1989**, *158*, 74-76. (c) Vogler, A.; Kunkely, H. *Chem. Phys. Lett.* **1988**, *150*, 135-137. (d) Kunkely, H.; Vogler, A. *Chem. Phys. Lett.* **1989**, *164*, 621-624.

(29) Russel, P. G. *J. Phys. Chem.* **1975**, *79*, 1347-1352.

(30) The relative photodegradation rates are estimated from the illumination times from a fixed illumination source required to decrease the absorption of Cd_n by 50% at the same extinction.

(31) (a) Henglein, A. *Ber. Bunsen-Ges. Phys. Chem.* **1982**, *86*, 301-305. (b) Meissner, D.; Memming, R.; Shuben, L.; Yesodharan, S.; Graetzel, M. *Ber. Bunsen-Ges. Phys. Chem.* **1985**, *89*, 121-124. (c) Baral, S.; Fojtik, A.; Weller, H.; Henglein, A. *J. Am. Chem. Soc.* **1986**, *108*, 375-378.

(32) Fischer, Ch.-H.; Henglein, A. *J. Phys. Chem.* **1989**, *93*, 5578-5581.

TABLE I: Redox Peak Potentials of Cd_n in CH_3CN as a Function of Cluster Size[a]

cluster	E_{ox},[b] V	E_{red},[c] V
Cd_1	0.88	[d]
Cd_4	0.77	−2.47
Cd_{10}	0.68	−2.02

[a] Ag/AgCl reference electrode. Scan rate = 200 mV/s. Both oxidation and reduction waves were chemically irreversible at all scan rates up to 200 V s^{-1}. The average deviation is determined to be ±10%. [b] Pt-disk working electrode. [c] HMDE working electrode. [d] Scanned to −2.8 V vs Ag/AgCl.

yields. Absorption and emission measurements were carried out with thianthrene, dibenzothiophene, and benzenethiol in CH_3CN in order to determine whether the absorption and emission spectra of the photolyzed Cd_n solutions may be attributed to a superposition of the absorption and emission spectra of these compounds. Thianthrene, dibenzothiophene, and benzenethiol all absorb at $\lambda < 330$ nm and show structured absorption spectra. However, a superposition of their absorption spectra matches the absorption spectrum of the Cd_n photodecomposition (Figure 3d). Furthermore, a superposition of the emission spectra of thianthrene and dibenzothiophene similarily matches the emission spectrum of the photolysis mixture formed upon illumination of Cd_n (Figure 4d): thianthrene and dibenzothiophene emit at 350 and 445 nm, respectively, following excitation at 290 nm. Benzenethiol shows no measurable emission. Furthermore, a yellowish precipitate was formed during the photolysis. According to ESCA, it was not CdS, but the possibility that elemental Cd was present could not be excluded.

Thus, from the MS, absorption, and emission data, we conclude that photolysis of Cd_n leads to the formation of thianthrene, dibenzothiophene, and benzenethiol. The insensitivity of the photodecomposition of the Cd_n clusters toward oxygen is consistent with the observation that none of the photoproducts contain oxygen.

The photolysis is certainly not a simple process as indicated by the product analysis. However, some reasonable assumptions can be made. The related compound $Hg(SPh)_2$ photodecomposes to mercury and SPh• radicals.[34] Owing to the LMCT nature of the reactive excited state, the $Cd(SPh)_2$ moiety may undergo a similar reaction as primary photoprocess. The secondary reactions could lead to product formation by the following overall stoichiometries:

$$Cd(SPh)_2 \rightarrow Cd + H_2 + \text{thianthrene}$$

$$Cd(SPh)_2 \rightarrow Cd + H_2S + \text{dibenzothiophene}$$

This suggestion is not unreasonable since Zn and Cd sulfur compounds are well-known to photocatalyze the dehydrogenation and subsequent carbon–carbon coupling of organic compounds.[35] The formation of thiophenol may result from hydrogen abstraction of the primary thiophenolate radicals.

Electrochemical Behavior of Cd_n: Redox Potentials as a Function of Cluster Size. The redox potentials of Cd_n are determined as a function of cluster size by cyclic voltammetry. For Cd_n, the oxidation is most likely sulfur centered and the reduction metal centered.[31c,32,36] All the Cd_n clusters show a broad oxidation wave which is chemically irreversible at all scan rates up to 200 V s^{-1}. The potential at which the oxidation occurs clearly depends on the cluster size (Table I): the oxidation peak potential is shifted to less positive values with increasing cluster size. A similar size dependence is observed for the reduction waves of Cd_n which are also chemically irreversible and rather broad: an increase in cluster size leads to a shift of the reduction peak potential to less negative values. Since the electrochemistry was irreversible, the significance of the data is not quite clear. However, the observed shifts in the redox potentials of Cd_n with cluster size are consistent with the size dependence of the optical properties of these clusters and in good agreement with theory.[1-4,6]

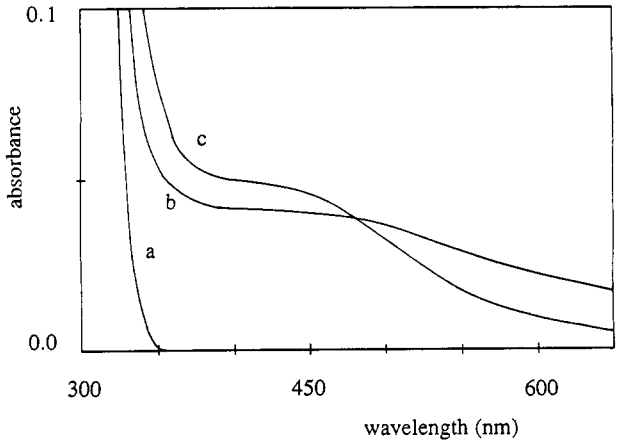

Figure 5. Charge-transfer complexes of Cd_4 (counterion Me_4N^+) and Cd_{10} (counterion Me_4N^+) with MV^{2+} (counterion PF_6^-) in aerated CH_3CN: (a) absorption spectrum of Cd_4, $c(Cd_4) = 2.7 \times 10^{-5}$ M; (b) absorption spectrum of Cd_4/MV^{2+}, $c(Cd_4) = 2.7 \times 10^{-5}$ M and $c(MV^{2+}) = 1.0 \times 10^{-2}$ M; (c) absorption spectrum of Cd_{10}/MV^{2+}, $c(Cd_{10}) = 5.2 \times 10^{-5}$ M and $c(MV^{2+}) = 4.5 \times 10^{-5}$ M.

Reaction with Methyl Viologen: Formation of Charge-Transfer Complexes. Both Cd_4 and Cd_{10} form ground-state charge-transfer (CT) complexes with methyl viologen (MV^{2+}) in CH_3CN as evidenced by the occurrence of a new broad absorption band upon addition of methyl viologen (Figure 5). The formation of ion-pair complexes between MV^{2+} and several anionic electron donors has been previously reported.[37] For Cd_4/MV^{2+}, the maximum of the CT complex is at ca. 470 nm, whereas Cd_{10}/MV^{2+} exhibits a maximum at ca. 440 nm (Figure 5).[38] In view of the redox potentials of the clusters (Table I), this observation seems to be surprising. However, this influence may be overcompensated by the outer-sphere reorganizational energy which also depends on the size of the redox centers.[37,39] This energy should increase from Cd_4 to Cd_{10}. Furthermore, a charge effect may be important as the ground-state charge for Cd_4/MV^{2+} (2−/2+) is different from that of Cd_{10}/MV^{2+} (4−/2+). A similar blue-shift in the absorption maximum of the CT complex upon increasing the (ground state) charge of the anionic electron donor has been recently reported for a series of CT complexes between methyl viologen and naphthalene derivates of different charge.[40] In the case of Cd_1, the methyl viologen radical cation ($MV^{\bullet+}$) is formed, either by thermal electron transfer or by photodecomposition of the extremely light-sensitive complex and subsequent reaction of the photoproducts with MV^{2+} yielding $MV^{\bullet+}$.[41]

Cd_4 forms a 1:1 complex with MV^{2+}. The complex formation equilibrium constant and the extinction coefficient (at 470 nm) of Cd_4/MV^{2+} are determined to be 5400 ± 500 M^{-1} and 880 M^{-1} cm^{-1}, respectively, applying the Benesi–Hildebrand method.[42] For Cd_{10}/MV^{2+}, precipitation occurs for $c(MV^{2+}) > c(Cd_{10})$. The complexation of Cd_{10} (ground-state charge 4−) with a second MV^{2+} molecule yielding a 1:2 complex leads to a charge neutralization of the adduct and subsequently to its precipitation. A

(33) MS of Cd_n was carried out as a control experiment and yielded different compounds: biphenyl-1,6-dithiol or phenyl disulfide (m/e = 218), biphenyl-4-thiol (m/e = 186), biphenyl (m/e = 154), and benzenethiol (m/e = 110). Thus, besides benzenethiol, MS of the Cd_n clusters leads to different products than are formed during photodecomposition. This suggests that benzenethiol might be also photochemically formed.

(34) Kern, R. J. *J. Am. Chem. Soc.* **1953**, *75*, 1865–1866.
(35) Kisch, H.; Künneth, R. *Photochemistry and Photophysics*; Rabek, J. F., Ed.; CRC Press: Boca Raton, FL, 1991; Vol. 4, pp 131–175.
(36) Kelm, M.; Lilie, J.; Henglein, A. *J. Chem. Soc., Faraday Trans. 1* **1975**, *71*, 1132–1142.
(37) Vogler, A.; Kunkely, H. *Top. Curr. Chem.* **1990**, *158*, 1–30.

(38) The exact positions of the maxima of the CT complexes are obtained from the second derivative of the absorption spectra of Cd_4/MV^{2+} and Cd_{10}/MV^{2+}.

(39) Powers, M. J.; Meyer, T. J. *J. Am. Chem. Soc.* **1980**, *102*, 1289–1297.
(40) Hubig, S. M. *J. Lumin.* **1991**, *47*, 137–145.
(41) Henglein, A. *J. Phys. Chem.* **1982**, *86*, 2291–2293.
(42) (a) Benesi, H. A.; Hildebrand, J. H. *J. Am. Chem. Soc.* **1949**, *71*, 2703–2707. (b) Deranleau, D. A. *J. Am. Chem. Soc.* **1969**, *91*, 4044–4049.

similar behavior, i.e., precipitation upon charge neutralization, is observed for many metal oxide colloids.[26,43] For Cd_{10}, the extinction coefficient of the 1:1 complex at 440 nm is determined to 1250 M^{-1} cm^{-1}, assuming complete conversion of Cd_{10}. Steady-state excitation of the CT complexes (λ_{ex} = 450 nm) of Cd_4 and Cd_{10} does not lead to the formation of $MV^{\bullet+}$, which is presumably caused by fast back electron transfer.

Conclusions

Three cadmium benzenethiolate clusters Cd_n (n = 1, 4, 10) of well-defined size and structure have been examined as molecular models for the semiconductor CdS and have been characterized by spectroscopic and electrochemical methods. Cd_n display structured absorption spectra which are assigned to both LMCT and intraligand transitions. For the polynuclear Cd_n clusters (n = 4, 10), the position of the absorption maxima clearly depends on cluster size; i.e., the absorption bands of Cd_{10} are red-shifted compared to those of Cd_4. Similarily, Cd_{10} emits at longer wavelengths than Cd_4. Emission from Cd_1 is not observed. The emission bands of Cd_4 and Cd_{10} are ascribed to MLCT transitions as suggested by their short luminescence lifetimes and the red-shift of the luminescence with increasing cluster size. The electrochemical properties of these Cd_n clusters show a similar dependence on cluster size: an increase in cluster size leads to both a shift of the oxidation wave to less positive potentials and a shift of the reduction wave to less negative potentials. The size-dependent optical and electrochemical properties of the Cd_n clusters are qualitatively in good agreement with theory.[1-4]

Photodecomposition of Cd_n, which is not affected by oxygen, yields thianthrene, dibenzothiophene, and benzenethiol. The rate of photodegradation also depends on cluster size; i.e., the photostability of the Cd_n clusters is enhanced with increasing cluster size. Cd_4 and Cd_{10} form ground-state charge-transfer complexes with the cationic electron acceptor methyl viologen, the position of the CT band depending on the size and charge of the anionic electron donor (the Cd_n cluster). However, steady-state illumination of the CT complexes does not lead to the formation of the methyl viologen radical cation.

Acknowledgment. We thank F. Sabin for help with the synthesis of the Cd_n clusters, Dr. J. Merkert for help with the electrochemical measurements, D. J. Kiserow and Dr. S. J. Atherton for help with the time-resolved emission measurements, and Drs. S. M. Hubig and B. A. Gregg for stimulating discussions. Financial support of the work at the University of Regensburg by the Deutsche Forschungsgemeinschaft and at the University of Texas by the U.S. Army Research Office is gratefully acknowledged. Initial SPC measurements were made at the Center for Fast Kinetics Research, a facility jointly supported by the National Institutes of Health and the University of Texas.

(43) Kormann, C.; Bahnemann, D. W.; Hoffmann, M. R. *J. Phys. Chem.* **1988**, *92*, 5196-5201.

A Local Dielectric Constant Model for Solvation Free Energies Which Accounts for Solute Polarizability

Kim Sharp, Arald Jean-Charles, and Barry Honig*

Department of Biochemistry and Molecular Biophysics, Columbia University, 630 W. 168th St., New York, New York 10032 *(Received: June 6, 1991)*

A model for treating solute polarizability in solvation processes is presented. The model, which requires little computation compared to atomic detail simulations, is based on a classical electrostatic treatment, whereby the solute polarizability is represented by local dielectric constants (LDC) rather than the usual point inducible dipoles. Point inducible dipoles and local dielectric constants are shown to be formally equivalent ways of representing solute polarizability for a simple spherical, point dipolar solute. For more realistic solute representations, however, there are some advantages to the local dielectric model. The solvation energy, change in solute dipole moment upon polarization, and the polarization energy in the LDC model are obtained self-consistently from one set of calculations involving solutions to the Poisson equation. Calculated solvation energies are compared to experimental data for water and 12 small polar solutes.

Introduction

Most available force fields that are used in molecular simulations do not treat electronic polarizability explicitly. This is due in large part to the computational expense associated with accounting for nonadditive pairwise interactions and to the theoretical difficulties associated with developing a valid model. Polarization effects are treated implicitly in that force-field parameters, such as charge and atomic radius, are generally chosen so as to reproduce experimental properties, but nevertheless, the neglect of polarizability imparts a degree of uncertainty to the conclusions that can be derived from simulations. In recent years a number of polarizable water models have been reported and have been used primarily to study pure water and ion-water interactions.[1-3] However, the same effort has not yet been invested in the treatment of solute polarizability. Since it is known that dipole moments change significantly in transfers from the gas phase to polar solvents, electronic polarizability makes an important contribution to solvation free energies. In this paper we develop a treatment of solute polarizability which is based on solving the Poisson equation for a solute molecule embedded in a solvent represented as a continuous medium.

Our treatment is based on classical dielectric models[4] which treat the solute as a cavity embedded in a dielectric medium. However, in contrast to earlier work, it is now possible to use numerical methods to account for the shape and charge distribution of the solute in atomic detail.[5] Comparisons with experiment and with the results of microscopic simulations of the solvent suggest that the continuum treatment offers comparable accuracy for many problems with orders of magnitude less computer time.[6-8] This has opened up the possibility of a simple, fast,

(1) Barnes, P.; Finney, J. L.; Nicholas, J. D.; Quinn, J. E. *Nature* **1979**, *282*, 459.
(2) Sprik, M.; Klein, M. L. *J. Chem. Phys.* **1988**, *89*, 7556.
(3) Dang, L. X.; Rice, J. E.; Caldwell, J.; Kollman, P. A. *J. Am. Chem. Soc.* **1991**, *113*, 2481-2486.
(4) Bottcher, C. J. F. *Theory of Electric Polarization*; Elsevier Press: Amsterdam, 1973.
(5) Sharp, K.; Honig, B. *Annu. Rev. Biophys. Biophys. Chem.* **1990**, *19*, 301-332.
(6) Rashin, A. A.; Honig, B. *J. Phys. Chem.* **1985**, *89*, 5588.

0022-3654/92/2096-3822$03.00/0